ResearchGate

See discussions, stats, and author profiles for this publication at: https://www.researchgate.net/publication/248161874

Tsunamis in the Mediterranean Sea

Article

CITATIONS
7

READS
785

1 author:

Gerassimos A. Papadopoulos
National Observatory of Athens
275 PUBLICATIONS 3,156 CITATIONS

SEE PROFILE

Some of the authors of this publication are also working on these related projects:

Project Earthquake prediction from short-term foreshocks View project

Project SEAHELLARC View project

All content following this page was uploaded by Gerassimos A. Papadopoulos on 27 July 2015.

The user has requested enhancement of the downloaded file.

17 Tsunamis

Gerassimos Papadopoulos

Introduction

According to Imamura (1937: 123), the term *tunami* or *tsunami* is a combination of the Japanese word *tu* (meaning a port) and *nami* (a long wave), hence long wave in a harbour. He goes on to say that the meaning might also be defined as a seismic sea-wave since most tsunamis are produced by a sudden dip-slip motion along faults during major earthquakes (Figure 17.1). Other submarine or coastal phenomena, however, such as volcanic eruptions, landslides, and gas escapes, are also known to cause tsunamis. According to Van Dorn (1968), 'tsunami' is the Japanese name for the gravity wave system formed in the sea following any large-scale, short-duration disturbance of the free surface. Tsunamis fall under the general classification of long waves. The length of the waves is of the order of several tens or hundreds of kilometres and tsunamis usually consist of a series of waves that approach the coast with periods ranging from 5 to 90 minutes (Murty, 1977). Some commonly used terms that describe tsunami wave propagation and inundation are illustrated in Figure 17.2.

Because of the active lithospheric plate convergence, the Mediterranean area is geodynamically characterized by significant volcanism and high seismicity as discussed in Chapters 15 and 16 respectively. Furthermore, coastal and submarine landslides are quite frequent and this is partly in response to the steep terrain of much of the basin (Papadopoulos *et al.* 2007*a*). Tsunamis are among the most remarkable phenomena associated with earthquakes, volcanic eruptions, and landslides in the Mediterranean basin. Until recently, however, it was widely believed that tsunamis either did not occur in the Mediterranean Sea, or they were so rare that they did not pose a threat to coastal communities. Catastrophic tsunamis are more frequent on Pacific Ocean coasts where both local and transoceanic tsunamis have been documented (Soloviev, 1970). In contrast, large tsunami recurrence in the Mediterranean is of the order of several decades and the memory of tsunamis is short-lived. Most people are only aware of the extreme Late Bronge Age tsunami that has been linked to the powerful eruption of Thera volcano in the south Aegean Sea (Marinatos, 1939) (Chapter 15). Even that wave is commonly not viewed as a significant geophysical event. Indeed, it is often seen as rather an exotic episode—part myth and part fact—given that it happened in prehistoric times and has been linked with the collapse of the Minoan civilization of Crete. These are some of the reasons why, in comparison to other parts of the world, the scientific study of tsunamis in the Mediterranean Sea has been rather neglected until the last few decades.

This chapter reviews the tsunami history of the Mediterranean and evaluates the progress that has been made in assessing the tsunami hazard over its several regions. In addition, the prospects for further development of tsunami science and associated risk mitigation technology in the region are outlined.

Tsunami Quantification

A parameter that is of particular importance for understanding tsunami-generating mechanisms and assessing tsunami hazard better is wave size, and this can be expressed as either intensity or magnitude. These parameters, however, are difficult to determine—even for more recent events (e.g. Soloviev, 1970; Shuto, 1993). In Europe, tsunami intensity (k) is traditionally estimated according to the 6-grade Sieberg-Ambraseys scale (Ambraseys, 1962). In this chapter,

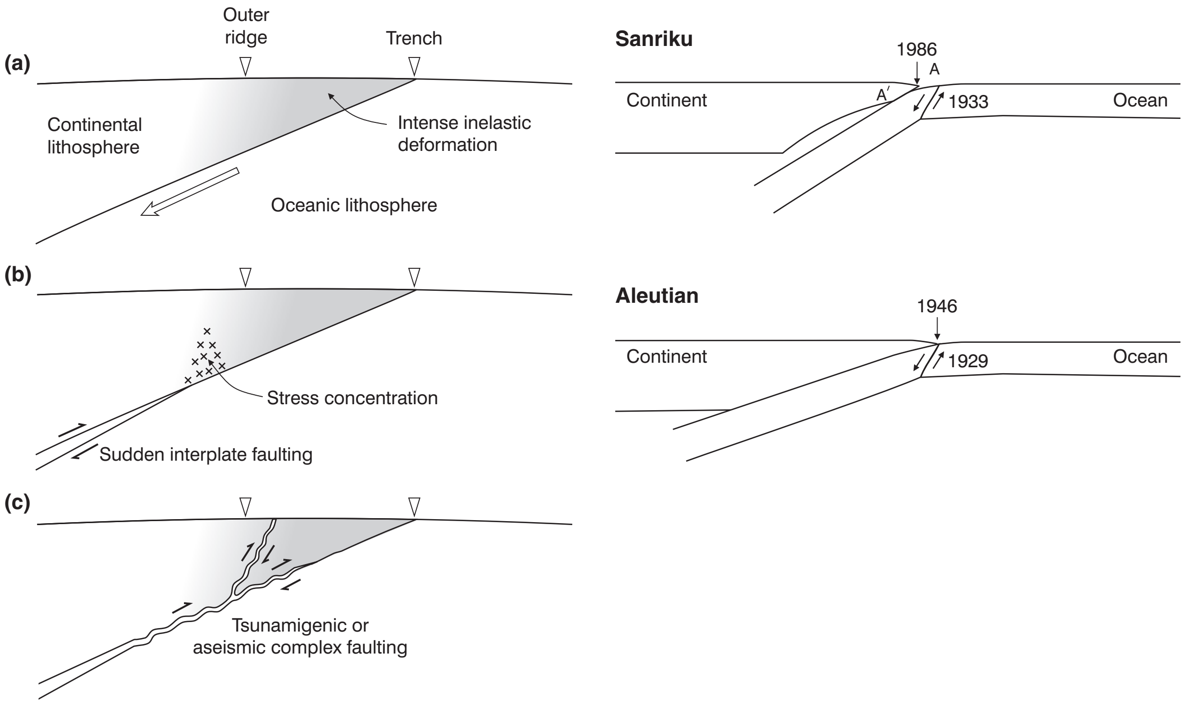

Fig. 17.1. Co-seismic dip-slip motion along faults and tsunamigenesis near deep sea trenches. The diagram on the left (after Fukao, 1979) shows the sequence (a–c) of inelastic deformation and stress concentration culminating in aseismic faulting. In the Sanriku (north-east Japan) and Aleutian examples, thrust faulting is assumed to be the mechanism responsible for the 1896 and 1946 tsunamigenic earthquakes, whilst normal faulting is assumed for the 1933 and 1929 events (modified from Kanamori, 1972).

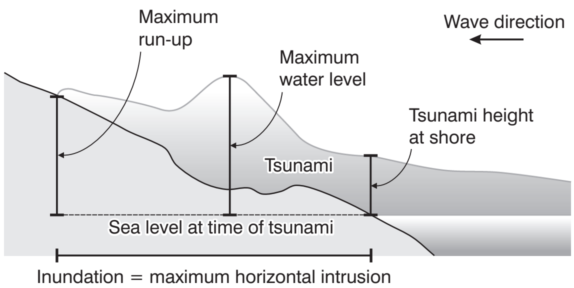

Fig. 17.2. A schematic explanation of some of the tsunami terms used in this chapter (modified from IOC, 1998).

the reported tsunami intensities are based on this scale, while the Murty-Loomis (1980) definition is adopted for tsunami magnitude (*ML*). An attempt has been made to recalculate the intensities of some important Mediterranean tsunamis according to a recently introduced 12-grade intensity scale (Papadopoulos and Imamura, 2001; Papadopoulos, 2003*a*) and these are shown in Table 17.1.

Major Tsunami Events in the Mediterranean

In this section the tsunami history of the Mediterranean Sea is reviewed. Emphasis is given to a selection of key tsunami events and these were chosen because of their significant impact on coastal communities and also because they have been extensively studied by a wide range of geophysical, geological, geomorphological, historical, and archaeological research methods as well as by hydrodynamic numerical modelling techniques. This review also aims to evaluate the advantages and disadvantages of the research methods that have been used, to highlight the progress achieved in this area, and to identify the emerging prospects for further research. The tsunami catalogues used in the following review are based mainly on those of Galanopoulos (1960), Ambraseys (1962), Antonopoulos (1979), Papadopoulos and Chalkis (1984), Tinti and Maramai (1996), Soloviev *et al.* (2000), Papadopoulos (2001, 2003b), Tinti *et al.* (2004) and Fokaefs

TABLE 17.1. *Strong tsunamis of intensity $k \geq 4$ reported for the Mediterranean Sea between 426 BC and AD 2002*

No	Year	Month	Day	Location	*k*	Ref	*K*	*h*(cm)	*ML*
1	426 BC	summer		Maliakos Gulf	5	P	8		
2	373 BC	winter		W. Gulf of Corinth	5	P	9		
3	142/4			Rhodes	4	P	7		
4	365	07	21	Crete	5	P	10		
5	447	01	26	Sea of Marmara	4	P	8		
6	551	07	09	Lebanon	5	**	8		
7	552	05		Maliakos Gulf	4	P	8		
8	556			Kos	4	P	8		
9	749	01	18	Levantine coast	4	**	7		
10	1169	02	04	Messina Straits	4	TM	8		
11	1202	05	20	Syrian coast & Cyprus	4	AM	7		
12	1303	08	08	Crete	5	P	10		
13	1343	10	18	Sea of Marmara	4	P	8	200	
14	1365	01	02	Algiers	4	**	8		
15	1389	03	20	Chios	4	P	6		
16	1402	06		Gulf of Corinth	4	P	8		
17	1481	05	03	Rhodes	4	**	7		
18	1609	04		Rhodes	5	P	8		
19	1612	11	08	Crete	4	P	8		
20	1627	07	30	Gargano, Italy	4	**	6		−1.4
21	1650	10	11	Thera	6	P	10	2,000	+3.0
22	1693	01	11	Eastern Sicily	4	TM	7		+2.3
23	1741	01	31	Rhodes	5	P	8		
24	1748	05	25	W. Gulf of Corinth	4	P	9	1,000	
25	1759	11	25	Akko	5	**	8		
26	1766	05	22	Sea of Marmara	4	P	7		
27	1773	05	06	Tangiers	4	**	7	900	
28	1783	02	06	Calabria	6	TM	9	900	−1.8
29	1817	08	23	W. Gulf of Corinth	4	P	9	500	
30	1823	03	05	North Sicily	4	TM	8		
31	1856	11	13	Chios	4	P	8		
32	1866	01	02	Albania	4	P	7		
33	1866	02	02	Kythira	4	P	6	800	
34	1866	03	06	Albania	4	P	7		
35	1867	09	09	Gythion	4	P	7		
36	1908	12	28	Messina Straits	6	TM	10	1,300	−0.4
37	1944	08	20	Stromboli	4	TM	7		
38	1948	02	09	Karpathos	4	P	7		
39	1956	07	09	Cyclades	6	**	9	1,500	+3.0
40	1963	02	07	W. Gulf of Corinth	4	P	7	500	−11.0
41	1979	04	15	Montenegro	4	P	8		
42	1999	08	17	Sea of Marmara	4	P	6	250	
43	2002	12	30	Stromboli	4	*	7	900	

Notes: k = tsunami intensity in the 6-grade scale of Sieberg-Ambraseys, K = tsunami intensity in the 12-grade scale of Papadopoulos and Imamura (2001), h = run-up height, *ML* = Murty-Loomis (1980) tsunami magnitude.
* new event.
** revised in this chapter.

Sources: AM = Ambraseys (1962), P = Papadopoulos (2001), TM = Tinti and Maramai (1996) and Tinti *et al.* (2004).

and Papadopoulos (2007). Tsunamigenic zones in the Mediterranean determined from historical data are shown in Figure 17.3a, while Table 17.1 lists the key characteristics of the known strong tsunamis ($k \geq 4$). A range of field evidence has been utilized to identify palaeotsunamis and this includes sedimentological, geomorphological, and archaeological data (Figure 17.3b). The following sections review the evidence for tsunami activity across the Mediterranean region beginning with the Alboran Sea in the west and moving eastwards.

Alboran Sea

According to documentary sources, the earthquakes in northern Algeria of 2 January 1365, 6 May 1773, and 21 and 22 August 1856 caused tsunamis of up to

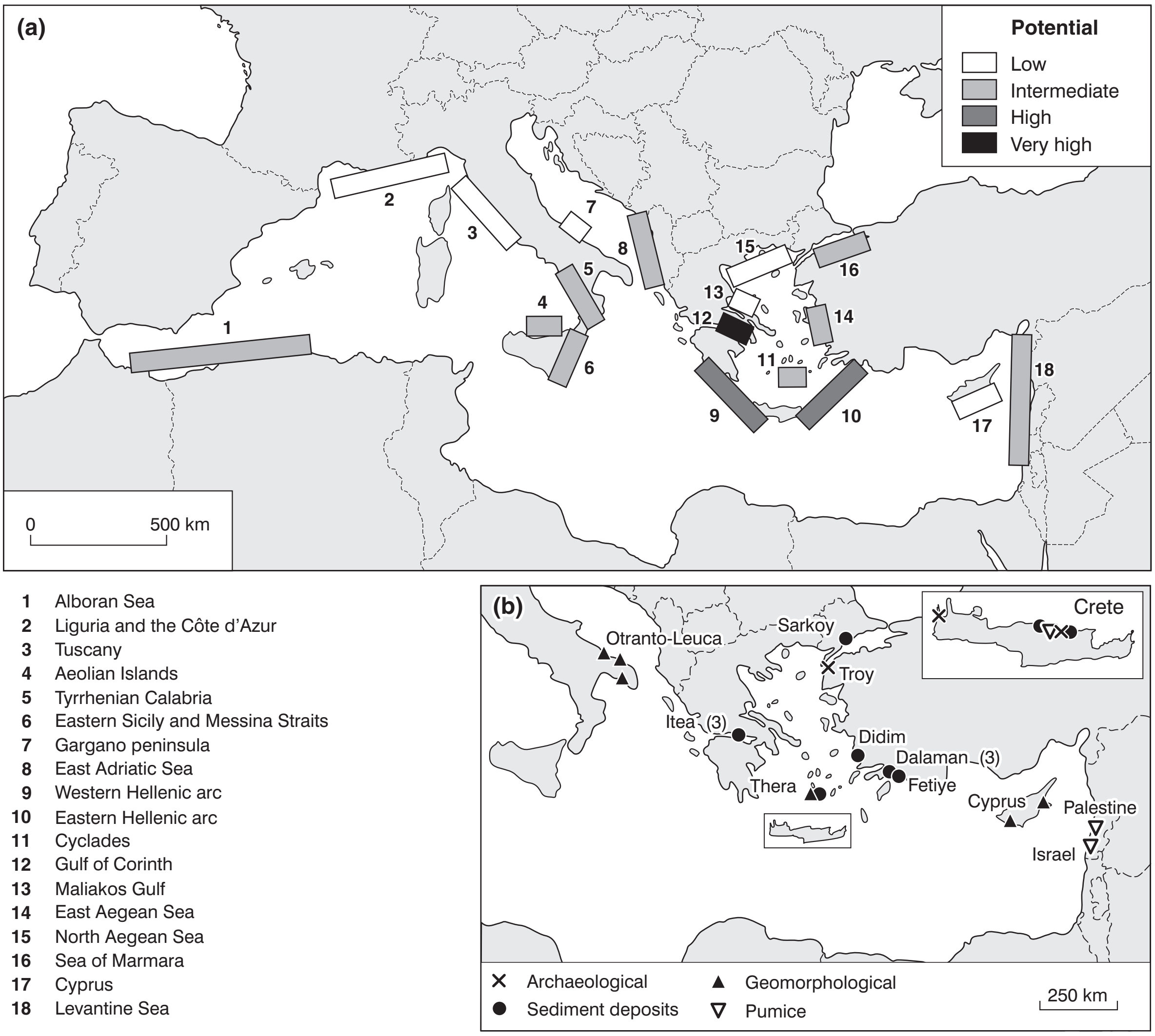

Fig. 17.3. (a) Tsunamigenic zones in the Mediterranean Sea defined from documentary sources and classified according to their relative tsunami potential as explained in the text. See also Table 17.1. Most of North Africa has not been classified. Here tsunami potential is generally regarded as being low and long-term records are not available. (b) Types of field evidence for the occurrence of past tsunamis.

k 4 (Figure 17.3a). Eyewitness accounts and tide-gauge records verify that similar tsunamis were produced by the strong earthquakes of 9 September 1954, 10 October 1980, and 21 May 2003. In these examples, the location of the earthquakes on land in northern Algeria produced submarine slumping that generated powerful turbidity currents (Soloviev *et al.* 2000). As a result, along the Spanish coast atmospheric gravity waves (*rissagas*) of up to 2-m amplitude and a frequency of about 10 minutes were observed. These waves have also been observed in southern bays of the Balearic Islands (Monserrat *et al.* 1991) and also in the Aegean Sea (Papadopoulos, 1993*a*).

Liguria and the Côte d'Azur

On 16 October 1979 a submarine slope failure that occurred during the construction of the new Nice airport produced a tsunami wave 3 m high that was observed near Antibes (Figure 17.3a). The near field wave heights were successfully simulated by Assier-Rzadkiewicz *et al.* (2000). The theoretical results were not, however, in complete agreement with the far field observations. This may be explained by the rapid amplitude attenuation of the tsunami due to strong wave dispersion, a common feature of landslide-generated tsunamis (Papadopoulos and Kortekaas, 2003; Papadopolous *et al.* 2007*a*). The 20 July 1564 and 23 February 1887 earthquakes (Eva and Rabinovich, 1997) triggered tsunamis inundating the coast from Nice to Antibes and from Genoa to Cannes respectively. A modern-day repeat of these intermediate magnitude waves would threaten the densely populated coastal zone of Liguria and the Côte d'Azur.

Tyrrhenian Sea

Along the coast of Tuscany in the northern Tyrrhenian Sea (Figure 17.3a), very few events have been reported since the *k* 4 tsunami of 5 March 1823. On the slopes of Stromboli in the Aeolian Islands (Figures 17.3a and 17.4), volcanic landslides produced tsunamis of *k* 3 or 4 on 3 July 1916, 22 May 1919, 11 September 1930, 20 August 1944, and 30 December 2002 (Figure 17.5). Further south an extreme event occurred in Tyrrhenian Calabria (Figures 17.3a and 17.4) on 6 February 1783 when a huge earthquake-induced rockfall triggered a *k* 6 tsunami at the Scilla beach (Tinti and Guidoboni, 1988). Inundation heights of 6–9 m were observed and more than 1,500 lives were lost. At Torre del Faro, to the north of Messina, the run-up height was about 6 m and twenty-six people were swept out to sea.

Eastern Sicily and the Messina Straits

The 11 January 1693 earthquake in north-east Sicily, that claimed about 70,000 victims, caused a tsunami of *k* 4. Sea-level oscillations destroyed many boats and ships while flooding was reported from Catania, Augusta, and Messina (Figures 17.3a and 17.4). Tinti *et al.* (2001) reported hydrodynamical studies of this event and concluded that the faults most likely to be the earthquake source are located in the Scordia-Lentini graben that intercepts the coastline.

The 28 December 1908 earthquake is one of the largest ever reported in Italy (Chapter 16). Major towns in southern Italy, including Messina and Reggio Calabria, were completely destroyed with more than 60,000 victims. The earthquake generated a violent tsunami in the Messina Straits (Figures 17.3a and 17.4). This tsunami consisted of at least three large waves that caused many deaths and severe damage to ships, buildings, and property. A tsunami of *k* 6 was observed along the Calabrian coast at Pellaro and on the Sicilian coast at S. Alessio where wave heights observed were 13 m and 11.7 m respectively. A tsunami with very similar characteristics to the 1908 event is believed to have struck the Messina straits in 1169.

A review of the seismological, geological, and geodetic data (Valensise and Pantosti, 1992) in association with information on tectonic stress inversion (Neri *et al.* 2004) indicates that the 1908 earthquake was associated with normal faulting (Chapter 16). However, the seismogenic fault has not yet been identified and this has hindered attempts to develop simulation models of this major Mediterranean tsunami.

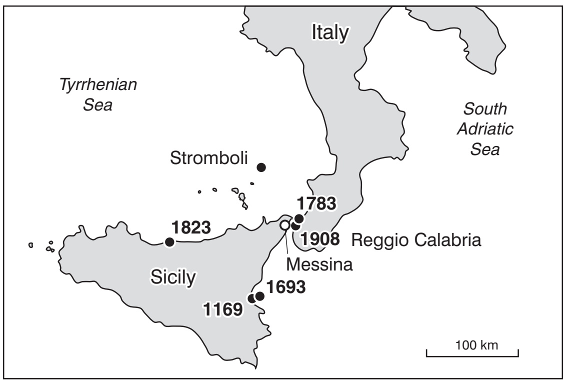

Fig. 17.4. Important tsunamis reported for southern Italy.

Adriatic Sea

Along the Adriatic coast of Italy, a tsunami source is related to the seismicity of the Gargano promontory (Figure 17.3a). The destructive earthquake of 30 July 1627, which may have been associated with the Apricena normal fault on land (Patacca and Scandone, 2004), caused a *k* 5 tsunami. Tinti *et al.* (1995) calculated that large events are expected in this area on average every 228 years. On the eastern side of the Adriatic Sea moderate to strong tsunami events were reported in Albania in 1866 and in Montenegro in 1979 (Figure 17.3a).

The Hellenic Arc

The large tsunamigenic earthquake of AD 21 July 365, located off the shore of western Crete (Papadopoulos and Vassilopoulou, 2001), is one of the most contentious and debated natural events in Mediterranean Sea history (Chapter 16). The accounts of Marcellinus, Athanasius, and Jerome, which are the closest in time to the event, leave no doubt that a large area was affected since the tsunami propagated to the north-west, west, and south of the Hellenic trench and reached as far as Methoni,

Fig. 17.5. Some of the damage caused by the Stromboli tsunami of 30 December 2002.

Sicily, Alexandria, and Dalmatia (Guidoboni *et al.* 1994; Ambraseys *et al.* 1994; Shaw *et al.* 2008) (Figures 17.3a and 17.6). Coastal uplift of up to 9 m in western Crete and 3 m in Antikythira (Thommeret *et al.* 1981; Pirazzoli *et al.* 1992) have been dated to (calibrated ages) AD 341–439 and 265–491, respectively. Therefore, the 365 event probably corresponds to the dramatic uplift event that raised the harbour at Phalasarna in northwest Crete, by *c.*6.6 m (Chapter 16).

In Phalasarna, tsunami deposits attributed to the AD 365 wave were described by Pirazzoli *et al.* (1992). According to Dominey-Howes *et al.* (1998), however, there is no biostratigraphical or lithostratigraphical evidence to infer tsunami sedimentary deposition. This may be due to the 6.6 m of uplift which could have taken place only a few minutes before the wave arrived if the uplift in western Crete and the AD 365 tsunami were caused by the same seismotectonic movement. Shaw *et al.* (2008) have recently argued that this earthquake took place not on the subduction interface beneath Crete, but on a fault with a dip of $c.30^\circ$ within the overriding plate. Their tsunami propagation calculations produced a damaging tsunami wave throughout the eastern Mediterranean with a repeat time of about 5,000 years for such an event. A range of archaeological, stratigraphical, geomorphological, and radiometric data imply that a tsunami struck Phalasarna after a strong earthquake around AD 66 (Pirazzoli *et al.* 1992; Dominey-Howes *et al.* 1998). In more recent times, remarkable earthquake tsunamis were also observed between the Peloponnese and Crete on 9 March 1630, 6 February 1866, and 20 September 1867.

Documentary sources indicate that the 8 August 1303 earthquake, which ruptured the eastern Hellenic arc between Crete and Rhodes (Figures 17.3a and 17.6), was one of the largest reported for the historical period in the Mediterranean. The most serious destruction was reported from eastern Crete (Guidoboni and Comastri, 1997) where a large tsunami struck Iraklion on the north coast. The sea swept violently into the city with such force that it destroyed buildings and killed inhabitants. In Acre, Israel, people were swept away and

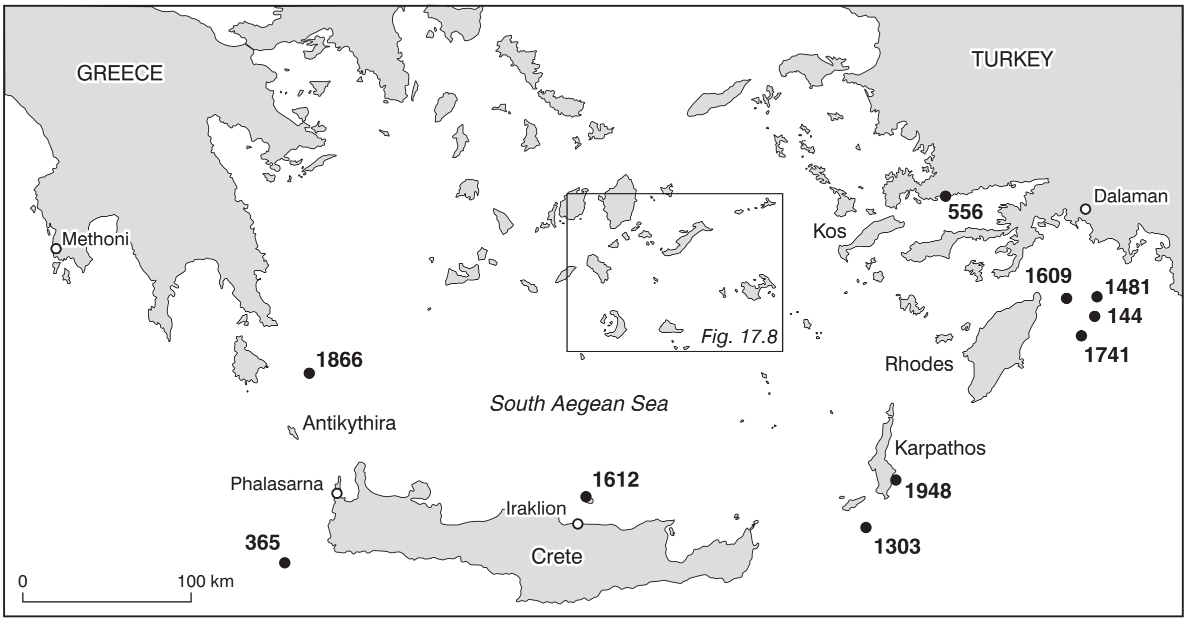

Fig. 17.6. Important tsunamis along the Hellenic arc. The Cyclades region (boxed area) is shown in greater detail in Figure 17.8.

drowned by a huge wave and in Alexandria the sea destroyed port facilities. In the easternmost Hellenic arc strong earthquake tsunamis occurred in AD 142 or 144 in Rhodes and Kos, AD 556 in Kos, 3 May 1481, April 1609, 31 January 1741, and 23 May 1851 in Rhodes, and 9 February 1948 in Karpathos (Figures 17.3a and 17.6). Trenches in Holocene sediments at Dalaman, south-west Turkey, have revealed three tsunami sand layers (Figure 17.7) attributed to the 1303, 1481, and 1741 tsunamis respectively (Papadopoulos *et al.* 2004). The 1609 wave, which violently inundated Rhodes, is missing from the Dalaman stratigraphy. This may be due to the fact that it failed either to penetrate this far inland or to leave a tsunami deposit at the location of the trench site.

The Cyclades

The Cyclades has a long record of tsunami events and is a key area for tsunami research (Papadopoulos *et al.* 2007*b*). The range of tsunami-generating mechanisms and the rich archaeological and sedimentary record of past tsunami activity mean that it is a key natural laboratory for the investigation of tsunami generation and their impacts.

The Minoan eruption is one of the most significant because of its size (Volcanic Explosivity Index = 6), its possible impact on Late Bronze Age (LBA) civilizations, and the distribution of huge amounts of tephra, thereby creating an important marker horizon around the eastern Mediterranean. The eruption history may have included four main phases (Heiken and McCoy, 1984) and concluded with the formation of the caldera that dominates the landscape of Thera (Santorini) (Figures 17.3a and 17.8) (Chapter 15). The most intensive eruption phase lasted for about 3–4 days (Sigurdsson *et al.* 1990). The Thera event has similarities with Krakatau where the collapse of the volcano-generated tsunamis that rolled against the shores of Java and Sumatra, with heights up to 35 m, leading to more than 36,400 casualties. From archaeological observations on Amnissos in northern Crete, Marinatos (1939) suggested that the Theran tsunami was linked with the demise of the Minoan civilization.

In coastal sites, assemblages of usually rounded pumice, often mixed with seashells, have been attributed to the Minoan tsunami. However, several cases are rather problematic. On Anafi Island, pumice layers at altitudes up to 250 m could not be attributed to Minoan tsunami deposition, as Marinos and Melidonis (1971) suggested, because the pumice there is at least 18,000 years old and of air-borne origin (Keller, 1978). Pumice found by Marinatos (1939) in Amnissos was linked to the Theran eruption without any analysis. The

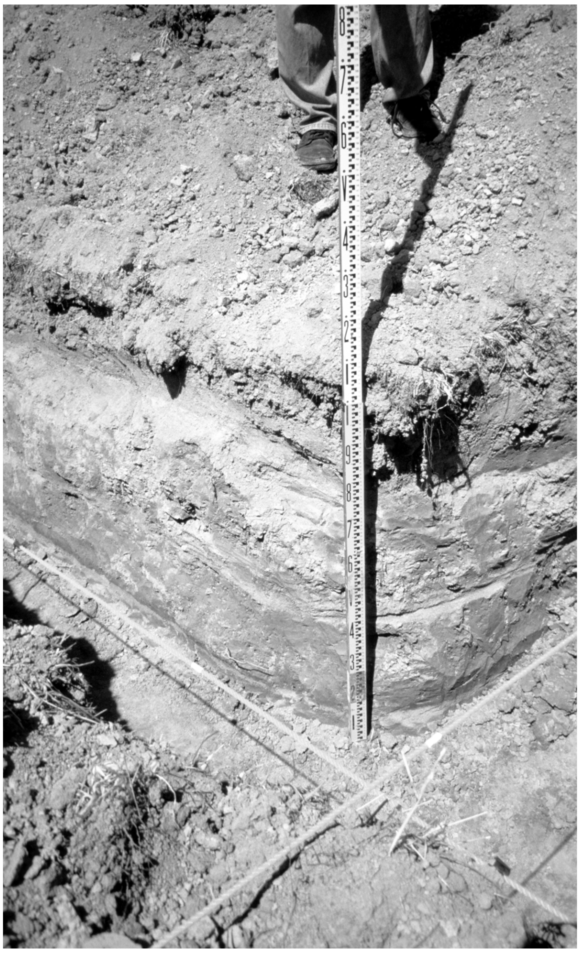

Fig. 17.7. An excavated section showing palaeotsunami deposits in Dalaman, south-west Turkey. This section was excavated in 1996 and was approximately 230 m from the present shoreline. Three tsunami sediment layers (dark colour) are present and these correspond to the 1303, 1481, and 1741 tsunamis in the east Hellenic arc.

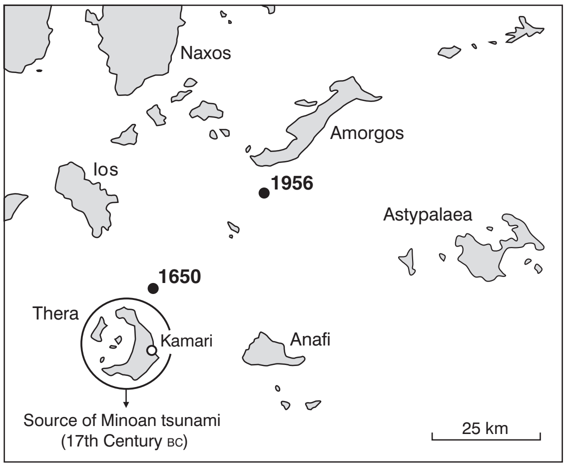

Fig. 17.8. Important tsunamis in the Cyclades islands in the southern Aegean Sea.

relationship between the Minoan tsunami and pumice deposits found in coastal sites of Cyprus, Israel, and Palestine is also rather speculative (Francaviglia, 1990).

Minoura *et al.* (2000) identified Minoan tsunami deposits in Gouves in northern Crete, and in coastal trenches in Didim and Fethye in south-west Turkey. AMS ^{14}C dating on fossil shells from Didim and on marine gastropod shells from Fethye, indicated that the eruption may have occurred around the second half of the nineteenth century BC and this places it about 200 years earlier than the previous estimates. In Thera, a 3.5-m thick volcaniclastic deposit intercalated with third and fourth phase deposits of the Late Bronze Age eruption has been interpreted as tephra reworked by the Minoan tsunami (McCoy and Heiken, 2000). Dominey-Howes (2004) found no evidence for any Late Bronze Age tsunami at forty-one coastal sites on Crete and Kos.

Futher evidence for the Minoan tsunami comes from the marine sedimentary record (Chapter 2). Seismic-reflection surveys in topographic lows of the western Mediterranean and Calabrian Ridges have shown a distinct, acoustically transparent, flat-lying layer, nicknamed 'homogenites'. These deposits occupy the uppermost part of the sediment column (Kastens and Cita, 1981) within a stratigraphic unit characterized by an upward fining grain size that implies deposition in a single event controlled by gravitational settling. Kastens and Cita (1981) calculated that the emplacement occurred between about 4,400 and 3,100 years BP, and that the homogenite was deposited from sediment transport induced by the Minoan tsunami. The thick and structureless homogeneous mud was later recognized in more than fifty gravity cores in a range of contrasting settings (Cita and Aloisi, 2000).

Mechanisms proposed for the Minoan tsunami include the entry into the sea of both pyroclastic and debris flows propagated in all directions around the island (McCoy and Heiken, 2000) along with caldera collapse combined with a large tectonic earthquake (Pararas-Carayannis, 1992). To simulate the wave hydrodynamically, Minoura *et al.* (2000) suggested a sudden volcano collapse, caldera formation, inrush of water into the caldera, and collision of water masses

Fig. 17.9. Palaeotsunami investigation within an archaeological excavation in St George, Thalassitis, Kamari, in eastern Thera. The arrow points to a distinctive sediment layer produced by a tsunami and highlights the area shown in more detail in Figure 17.10.

with the caldera wall. Their simulation resulted in wave heights of >15 m in the near-field zone and of 6–11 m in northern Crete. However, the extent of the wave inundation was only several hundred metres and, although the fishing and trading economy could have been affected by the destruction of boats and harbour installations, it can be argued that a tsunami of this size would have had little long-term influence on the Minoan civilization.

Another large tsunami was generated during the eruption of Columbo, a submarine volcanic edifice lying 7.3 km to the north-east of Thera (Figure 17.8). The main volcanic activity began on 26th September 1650, while volcanism on 30 September was followed by a pause in activity. During this pause a sea swell encircled the whole of Thera island and the tsunami inundated the eastern coast and swept away churches, enclosures, boats, trees, and agricultural land. On the east and west coast of Patmos island and on Ios island, tsunami run-up heights of 30, 50, and 16 m respectively were reported. Ships and fishing boats moored at Iraklion were swept violently offshore, while vessels were crushed when the wave overtopped the city walls. The volcanic and seismic quiescence that prevailed before the tsunami struck implies that it was generated by submarine landsliding or collapse of the volcanic cone rather than by a strong earthquake or volcanic explosion (Dominey-Howes *et al.* 2000). A geological record of the 1650 tsunami has been recognized from the coastal site of St George's near Kamari village in eastern Thera (Figures 17.9 and 17.10). However, Dominey-Howes *et al.* (2000) were unable to trace any tsunami deposit signature across three trenches, one of them being only 500 m from the St George'site. The non-volcanic clasts they found were angular to very angular in form and it is therefore thought that the non-volcanic sediments may reflect local colluvial processes. Thus, alternative hypotheses involving discontinuous sediment deposition

Fig. 17.10. Detail of the tsunami deposits (dark layer) exposed in the section shown in Figure 17.9 and attributed to the 30 September 1650 volcanigenic tsunami. Note the pen in middle of the photograph for scale.

and overestimation of the event's magnitude have been considered (ibid.).

The most recent large Mediterranean tsunami occurred in the Cyclades (Figure 17.3a) on 9 July 1956 after a M_s 7.4 crustal earthquake associated with normal faulting (Papadopoulos and Pavlides, 1992; Chapter 16). The tsunami-generating rupture was about 100 km in length within the NE–SW trending basin formed by the Thera, Amorgos, and Astypalaea islands (Papazachos *et al.* 1985). Initial estimates of the near-source wave height varied between 15 and 30 m in Amorgos and Astypalaea (Galanopoulos, 1957; Ambraseys, 1960) (Figure 17.8). Four people drowned and extensive destruction was noted in port facilities and in both small and large vessels as well as on cultivated land and other property.

Two interrelated problems arise out of the study of the 1956 tsunami. The first is the generation mechanism and the second is that numerical simulations have failed to reproduce the observed wave heights accurately. From tide gauge records Galanopoulos (1957) and Ambraseys (1960) concluded that the wave was probably produced by co-seismic landslides. Submarine geophysical survey showed normal faulting in the sides of the Amorgos basin as well as sea floor sediment instability and a geologically very recent slump (24×6 km in area and 3.6×10^6 m^3 in volume) occupying part of the basin (Perissoratis and Papadopoulos, 1999). The proximity of the slumped area to the earthquake epicentre implies seismic ground accelerations much higher than the minimum values required to initiate slumping. The slump episode may have occurred in association with the 1956 earthquake. Numerical simulations showed a discrepancy by a factor of 3–10 between the maximum reported (30 m) and simulated (3–10 m) wave amplitudes at the source region (e.g. Yalçiner *et al.* 1993). Field observations and interviews with eyewitnesses (Dominey-Howes, 1996; Papadopoulos *et al.* 2005) showed that the wave amplitude may not have exceeded about 15 m in Astypalaea. Therefore, part of the discrepancy could be explained by an overestimation of the initially reported wave height. Nonetheless, a significant discrepancy remains unexplained. Thus it may be concluded that an adequate reproduction of the near-field wave amplitudes requires not only co-seismic sea-floor fault displacement but also an additional tsunamigenic component such as that from a co-seismic, massive submarine sediment slump.

The Gulf of Corinth

The Gulf of Corinth is especially prone to tsunamis due to high seismicity, steep bathymetry and a susceptibility to coastal landsliding (Papadopoulos, 2003*b*; Papadopoulos 2007*a*). It is shown on Figure 17.3 as having the highest tsunami potential in the Mediterranean region. In 373 BC it has been argued that the town of Helike, located about 7 km east of modern Aeghion (Figure 17.11a), was destroyed by an earthquake and tsunami (Guidoboni *et al.*, 1994; Papadopoulos, 1998; and see Chapter 16 for further discussion). Ten Spartan ships at anchor close by were destroyed. The lethal earthquakes of 25 May 1748 and 23 August 1817 generated similar tsunamis in Aeghion causing human losses and extensive damage to vessels, port facilities, and cultivated land. The June 1402 tsunami was also of high intensity and followed a large, possibly near-shore earthquake (Papadopoulos *et al.* 2000). Interestingly, the near-shore earthquake of 26 December 1861, having a magnitude comparable to the previous events, produced a tsunami of much lower intensity.

Seismically triggered earth slides caused local tsunamis along the north coast on 11 June 1794, 6 July 1965, 11 February 1984, and 15 June 1995. An aseismic tsunami generated by sediment slumping at

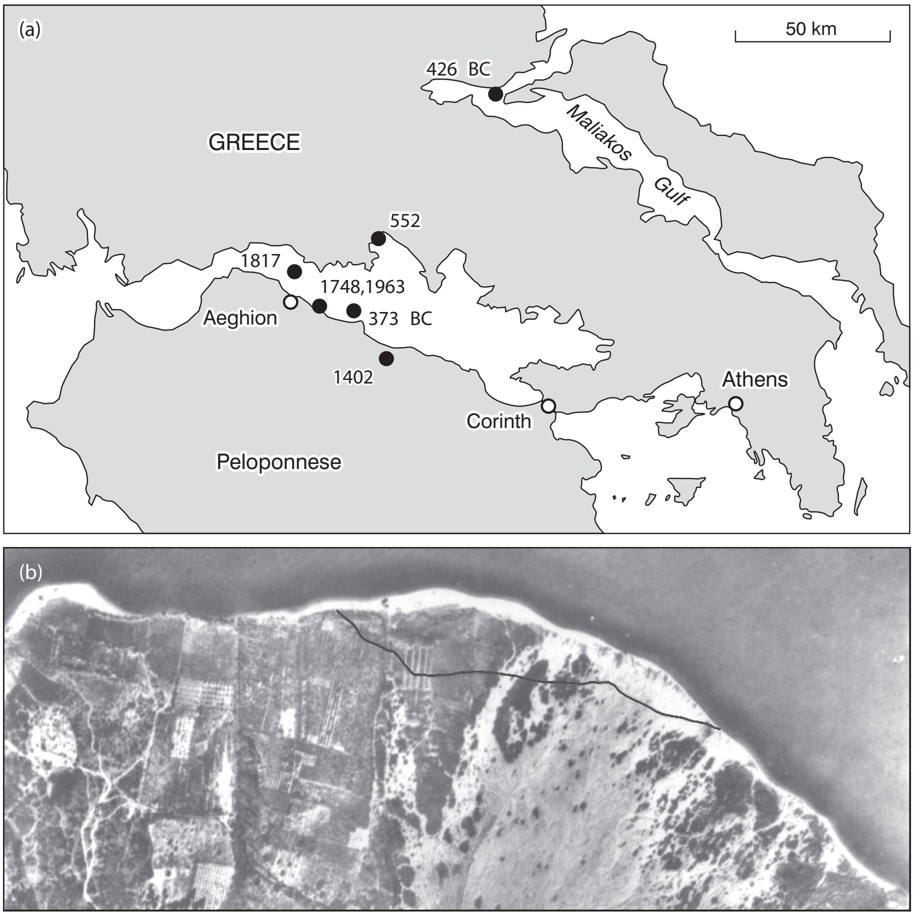

Fig. 17.11. (a) Important tsunamis in the Gulf of Corinth and the Maliakos Gulf. (b) An air photograph showing the coast prior to the large landslide that produced a tsunami in the west of the Gulf of Corinth on 7 February 1963 (after Galanopoulos *et al.* 1964). The black line marks the extent of the sediment mass that slipped seawards.

a river mouth hit both coasts at the western end of the Gulf of Corinth on 7 February 1963 (Figure 17.11b). The wave killed two people, injured twelve, and was responsible for serious damage to houses, cultivated land, and fishing boats (Galanopoulos *et al.* 1964). Numerical modelling results are consistent with run-up and inundation observations (Koutitas and Papadopoulos, 1998). A similar wave of lesser intensity was observed near Aeghion on 1 January 1996.

The Maliakos Gulf

The Maliakos Gulf is located on the western side of the Aegean and strong earthquake-generated tsunamis have been reported here for 426 BC and AD 551 or 552 from classical sources and archaeological evidence (Figures 17.3a and 17.11a). Records of past tsunami activity are not always consistent and care must be taken in their interpretation. For example, Papaioannou *et al.* (2004) suggested that the 426 BC event was, in fact, rather moderate and they argue that the large tsunami from this period may have occurred during the third century BC and that previous researchers amalgamated the two events into the earlier one at 426 BC. The Byzantine writer Procopius reported on an earthquake that struck the Gulf of Corinth in AD 551. He also described a strong tsunami in the Maliakos Gulf. However, it seems that Procopius did not actually describe a tsunami caused by the AD 552 earthquake, instead he just reproduced the classical sources detailing the 426 BC tsunami.

East and North Aegean Sea

A distinctive tsunami-prone region is associated with an earthquake zone around Chios Island in the eastern Aegean Sea (Figure 17.12a). Tsunamis of *k* 3 or 4 were observed on 20 March 1389, 12 May 1852, 8 September 1852, 13 November 1856, 2 February 1866, 3 April 1881, and 23 July 1949. Based on the writings of the Greek historian Democles (fourth century BC), some catalogues list a tsunami that supposedly struck Troy in about 1300 BC. A relevant passage in the *Wall War* of *Iliad* has not attracted much attention to date. In fact, rhapsody M18–19 describes how the wall of Greeks was damaged by river flooding, yet in M26–33 it becomes clear that the sea contributed to this destruction. In fact, the wall was inundated by the sea and trees and wall materials were carried away by the water; the ground was levelled by the strong wave and the coastal zone was covered by sand; while the sea caused the flow of rivers to reverse. The vivid descriptions in the *Iliad* indicate that a palaeotsunami survey along the coast of Troy could potentially be of great geomorphological and archaeological interest.

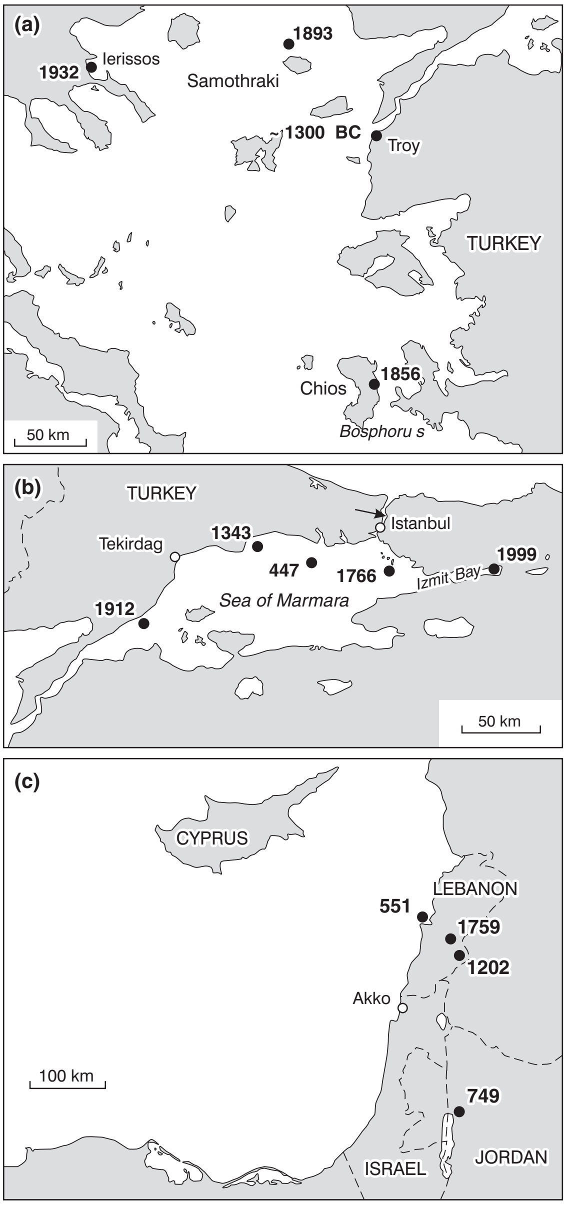

Fig. 17.12. Important tsunamis in (a) the east and north Aegean Sea, (b) the Sea of Marmara, and (c) the Cyprus–Levantine Sea area.

In the northern Aegean Sea (Figures 17.3a and 17.12a), a destructive wave that reportedly struck Potidaea on the Chalkidiki peninsula, in April 479 BC may imply tsunami action. This is the first tsunami described in documentary sources anywhere in the world. In AD 544 an earthquake-induced destructive inundation hit the coast of Thrace. More recently, seismic tsunamis of *k* 3 were observed in this area on Samothraki Island on 9 February 1893 and at Ierissos, Chalkidiki, on 26 September 1932.

The Sea of Marmara

This area has a long record of tsunami activity and *k* 3 or 4 tsunamis were caused by earthquakes on AD 26 January 447, 26 October 740, 2 September 1754, and 19 April 1878 in Izmit Bay. Tsunamis of *k* 3 or 4 were also caused by earthquakes on AD 25 September 478, 10 August 1265, 18 October 1343, 25 May 1419, 10 September 1509, and 10 July 1894 in Constantinople (Istanbul) as well as on 22 May 1766 in the Bosporus Straits, and on 9 August 1912 in Terkirdağ (Figures 17.3a and 17.12b). Due to higher seismicity, the east is the most tsunami-prone side of the Marmara Sea. The large (M_w 7.4) Izmit earthquake of 17 August 1999, caused by right-lateral strike-slip faulting with a significant normal component, generated damaging waves up to 2.5 m high in Değirmendere on the south coast, and elsewhere (Yalciner *et al.*, 2002) with intensities up to 4 (Papadopoulos, 2001). Rothaus *et al.* (2004) argued that the uniformity of the tsunami impact, indicating a wave coming to the south coast from 310°, suggests that submarine faulting was the major source of these tsunamis.

Cyprus-Levantine Sea

The final part of this review looks at the coasts bordering the Cyprus and Levantine Sea in the eastern Mediterranean. Archaeological excavations in Kourion, south-west Cyprus (Figures 17.3a and 17.12c), have revealed a destruction horizon attributed to the AD 21 July 365 earthquake tsunami that supposedly devastated Kourion (Soren, 1988). However, an earthquake location off the shore of south-west Cyprus is not consistent with both the AD 365 seismic damage distribution and tsunami wave propagation to the south, west, and north-west of Crete (Figure 17.6). An alternative explanation has been put forward that Kourion was hit by a non-tsunami-generating earthquake around AD 370 (Ambraseys, 1965; Guidoboni *et al.* 1994). In Cyprus, earthquake tsunamis were reported on 22 May 1201 or 1202, 11 May 1222, and 10 September 1953, the first two being of high intensity. Geomorphic evidence along coastal sections of southern Cyprus and radiocarbon dating results indicate tsunami activity between 1530 and 1821 (Whelan and Kelletat, 2002).

In the left-lateral strike-slip Levantine rift, tsunami-generating earthquakes have been identified from historical records (Figures 17.3a and 17.12c). On 9 July 551 the sea retreated for a mile and many ships were destroyed along the coasts of Lebanon, Syria, and Palestine, while after an earthquake on AD 18 January 749, the waves 'rose up to the sky' and destroyed most of the cities and villages along the coasts of Israel, Palestine, and Syria (Guidoboni *et al.* 1994, Darawcheh *et al.* 2000). Similar tsunamis were reported after strong earthquakes on 5 December 1033 (that shook the region around the Jordan Valley), on 29 May 1068 (an event possibly centred to the south of the Levantine rift), and on 14 January 1546 near the Dead Sea (Ambraseys *et al.* 1994).

Tsunami Generation Mechanisms

The large propagation areas of waves such as those of AD 365 and 1303 events leave little doubt that they were produced by co-seismic, sea-bottom dip-slip faulting. However, with only limited data about other tsunamis associated with large earthquakes of dip-slip faulting—such as the 1908 event in the Messina straits and the 1956 event in the Cyclades—it is often difficult to distinguish between co-seismic, landslide, or combined source mechanisms. In addition, the generation of tsunamis with strong local effects by earthquakes occurring on land—such as along the strike-slip Levantine rift—remains unexplained. Submarine landsliding triggered by powerful seismic shaking is a possibility, but an alternative mechanism is the dynamic excitation of tsunamis due to seismic energy transmission to the continental shelf by the vertical component of the long-period Rayleigh waves. However, in the highly seismogenic Cephalonia–Lefkada system of strike-slip faulting in the Ionian Sea, the tsunami activity is low—and in the Sea of Marmara, the tsunami potential is only intermediate (Figure 17.3a). This may be due to the fact that the earthquake focal mechanism involves mainly a strike-slip rather than a dip-slip component, while earth slumping may contribute to more local tsunami generation.

Volcanic eruptions are much less frequent than earthquakes in the Mediterranean and only a few tsunamis are therefore attributed to volcanic activity (Chapter 15). However, two of the largest known tsunamis were generated by strong eruptions in the Thera volcanic complex—namely the seventeenth-century BC Minoan tsunami and the AD 1650 Columbo tsunami. The generation of the Minoan tsunami may have included several mechanisms including caldera collapse, strong earthquake activity, pyroclastic surges and flows, and lahars and debris flows into the sea. Additional mechanisms that are worthy of more research include tsunami generation from atmospheric pressure changes due to the volcanic eruption, as well as abrupt sea-bottom impulse following the caldera collapse. The Columbo tsunami was probably caused by the partial collapse of the submarine caldera. Local but strong tsunamis caused by landsliding during eruptive activity of Stromboli have been reported repeatedly (Chapter 15).

Aseismic submarine or coastal landsliding is an important agent of locally powerful tsunamis (Papadopoulos *et al.* 2007*a*). The physiographic features of the Gulf of Corinth favour these processes and the most recent events were observed in 1963 and 1996. In the western Mediterranean in 1979, the collapse of a mass of unconsolidated artificial embankment into the sea in Nice on the Côte d'Azur, caused a local tsunami of similar character to that of 1963 in the Gulf of Corinth. Both events produced a large amplitude wave leading to loss of life and significant destruction in the near-source coastal zone.

Tsunami Hazard

This section evaluates tsunami hazard in Mediterranean coastal regions using four independent approaches. The first is a comparative description of the spatial distribution of tsunami events based on the geological

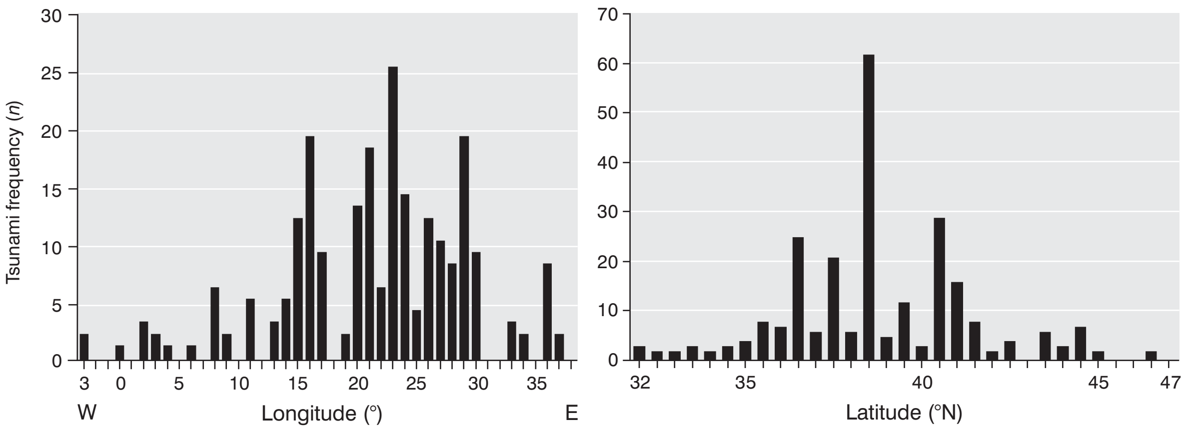

Fig. 17.13. The frequency (n) of tsunamis in the Mediterranean Sea as a function of longitude (left) and latitude (right) for the period 1628 BC to AD 2003.

and historical tsunami record over the last 3.5 millennia. Second, tsunami recurrence is calculated from empirical intensity–frequency relationships. The third is a statistical approach to estimate tsunami potential in a uniform way across the several tsunamigenic zones of the Mediterranean Sea. Finally, the occurrence of tsunamis is examined as a function of earthquake size. The data sets used here come from the various tsunami catalogues listed in the earlier sections.

The known tsunami sources in the Mediterranean are concentrated in eighteen zones of high seismicity and/or volcanism as shown in Figure 17.3a (Chapters 15 and 16). In the Mediterranean as a whole, the tsunami hazard (in terms of the event count) increases gradually from west to east—again tracking the basin-wide pattern of seismicity—although a decrease is apparent in the easternmost part of the basin. In fact, maximum activity occurs between 20°E and 30°E in the complex tectonic terrain and highly seismically-active structures of Greece (Figure 17.13) including the western and eastern segments of the Hellenic arc and the Gulf of Corinth. Significant tsunami activity is also concentrated in the seismic and volcanic region of Italy between 15°E and 17°E. The main belt of tsunami activity lies within a latitudinal zone between approximately 37°N and 41°N, which includes Greece, the Marmara Sea, the Tyrrhenian Sea, and southern Italy (Figure 17.13).

To determine the frequency of tsunami occurrence, some authors have used the intensity–frequency relationship:

$$\log N_c = \mathrm{a_c} - \mathrm{b}k \tag{1}$$

where N_c is the cumulative number of events of intensity equal to or larger than k observed in a time interval of c years, and a_c and b are parameters determined by the data. Equation (1) is analogous to the classic earthquake magnitude–frequency relationship (Gutenberg and Richter, 1944) and applies to tsunami-prone regions where relatively good datasets are available. For $c = 1$ formula (1) becomes:

$$\log N = a - bk \tag{2}$$

where:

$$a = a_c - \log c \tag{3}$$

Then, the mean tsunami recurrence for intensity $\geq k$ is equal to:

$$T = 10^{b\,k-a} \tag{4}$$

The most likely maximum tsunami intensity (k_t) expected in a time interval of t years is given by:

$$k_t = (a + \log t)/b \tag{5}$$

However, the small number of data points does not allow the application of this relationship in most of the tsunami-prone areas of the Mediterranean. Thus, this approach may only be applied in the larger tsunamigenic regions such as Greece, Italy, and the entire Mediterranean Sea. From the temporal distribution of the reported tsunami events a complete record for events of $k_c \geq 3$ from AD 1600 onwards is assumed (Figure 17.14). The results are shown in Figure 17.15 and Table 17.2 and suggest that, in the entire Mediterranean, the mean recurrence interval for tsunamis of

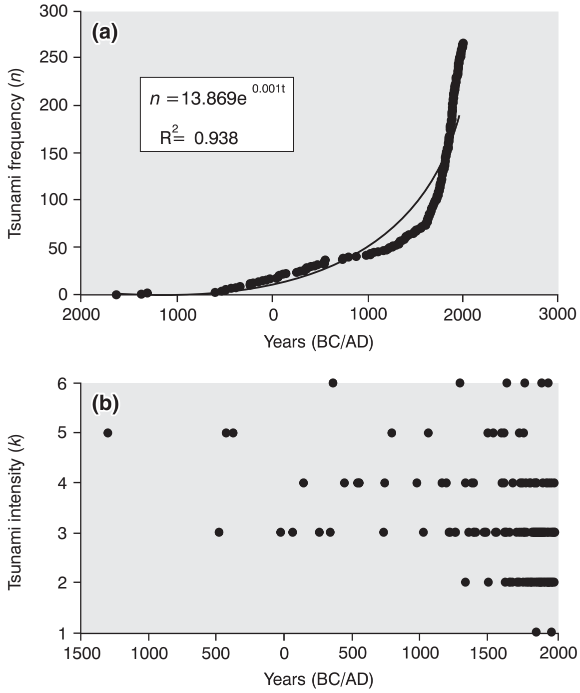

Fig. 17.14. The cumulative frequency (n) and intensity (k) of Mediterranean Sea tsunamis as a function of time for the period 1628 BC to AD 2003.

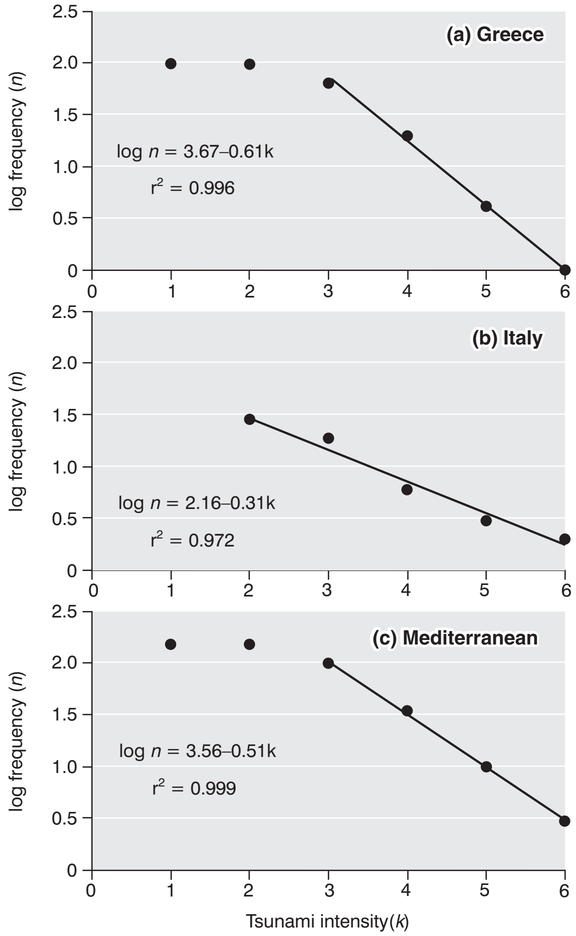

Fig. 17.15. Diagrams showing the relationship between intensity and frequency of tsunamis from the database for (a) Greece, (b) Italy, and (c) the Mediterranean Sea.

$k_c \geq 3$, 4, 5, and 6 is 4, 12, 40, and 130 years, respectively. This analysis also shows that Greece is characterized by a higher tsunami frequency than Italy, with the exception of k 6 events, which appear to recur more frequently in the Italian region. This last outcome, however, should be treated with some caution since it is based only on the post-1600 statistics and some very significant high intensity events, like the AD 365 and 1303 tsunamis in the Hellenic arc and the 1402 event in the Gulf of Corinth, were not considered in the calculation.

TABLE 17.2. *Mean return period (T) of tsunami intensity (k) and the most likely maximum tsunami intensity (k_t) to be observed in time interval t for various parts of the Mediterranean Sea*

Region	T (years)				k_t		
	$k \geq 3$	4	5	6	t(yrs) = 1	10	100
Mediterranean Sea	4	13	41	132	2	4	6
Greece	6	24	98	399	2	4	5
Italy	26	55	115	242		2	5
Gulf of Corinth*	40	103	261	662		2	4

* Modified from Papadopoulos (2003*b*).

Since detailed intensity-frequency relationships are impossible to obtain in most tsunami-prone regions due to small datasets, an alternative procedure was introduced for the uniform assessment of tsunami potential. This procedure combines information on the frequency and intensity of events, but does not consider the potential hazard to far-field locations which is due to wave propagation in remote places. Thus, the tsunami potential or hazard (H) of a particular zone or area is defined as the normalized quantity:

$$H = H_a / H_{min} \tag{6}$$

where the absolute potential, H_a, is an increasing function of the weighted event intensity and the event frequency:

$$H_a = \sum_{i=1}^{n}(k_{ci} \times j_c)/t_c$$

where $H_{min} = \min\{H_a\}$, k_{ci} is the intensity of event i, and j_c is a weighted factor of k_c. Factor j_c has been defined to follow a power law of base 2:2^1 for $k_c = 3$, 2^2 for $k_c = 4$, 2^3 for $k_c = 5$, and 2^4 for $k_c = 6$. Only events of $k_c \geq 3$ were considered. The lower date of the time interval (t_c) over which the data set is complete is variable, while the upper date was fixed at the end of 2003. The earliest event in the record was assumed to be AD 300 for $k_c = 6$, AD 1000 for $k_c = 5$, AD 1600 for $k_c = 4$, and AD 1750 for $k_c = 3$ (Figure 17.14). Equation (6) produces a relative tsunami potential scale with a minimum value equal to 1.

The eighteen tsunamigenic zones in the Mediterranean were classified into four groups of potential and these are shown in Figure 17.3a and Table 17.3. The lowest potential was found in Tuscany ($H = 1$), while low potential characterizes the coastal region from Liguria to the Côte d'Azur and the north Aegean Sea. The potential may be described as intermediate in the Alboran Sea, the Aeolian Islands, the Tyrrhenian Calabria, eastern Sicily, and the Messina straits, the Gargano promontory, the coasts of Albania and Montenegro, the Cyclades, the eastern Aegean Sea, the Sea of Marmara, and the Levantine Sea. High potential values were determined for the western and eastern segments of the Hellenic arc, while the Gulf of Corinth is classified as having the highest tsunami potential ($H = 12.83$) in the Mediterranean Sea (Figure 17.3a; Chapter 13).

In such regions as Cyprus, the Maliakos Gulf, the central and northern Ionian Sea, as well as Ionian Apulia and Calabria, only a few strong or moderate tsunamis have been documented—but these took place before the time period of complete data sets used in the above analysis. A characteristic example is the tsunami wave of intensity k 4 of AD 1222 in Cyprus (Fokaefs and Papadopoulos, 2007). In these regions the tsunami potential is not negligible, but it is impossible to quantify at present using the methods outlined above. Thus, these regions are provisionally classified as being of very low tsunami potential. The tsunami database for much of the North African coast of Tunisia, Libya, and Egypt is also very patchy and this probably reflects a combination of low tsunami potential (due to lower relief and low seismicity) and limited documentary and archaeological records.

It is important to appreciate that the intensity of an individual tsunami depends on many factors including earthquake size and epicentral location as well as the nature of the crustal displacement (Loritao *et al.* 2008) The local and regional sea floor bathymetry is also important—as is the geomorphology of the coastal zone receiving the tsunami wave. Given the range of variables, it is not surprising that there is not a strong correlation between tsunami intensity and earthquake magnitude and intensity (Figure 17.16). However, it is possible to identify an upper bounding envelope in both diagrams which shows that tsunami intensity does not exceed a certain value unless it is generated by an earthquake that exceeds a minimum size. For example, to produce a tsunami with an intensity ≥ 4 requires at least an earthquake magnitude of 6.3 or an earthquake intensity of 7.

TABLE 17.3. *Tsunami potential in each of the tsunamigenic zones of the Mediterranean shown in Figure 17.3a*

No in Fig. 17.3a	Region	H_a	H	Potential
3	Tuscany	0.024	1	low
7	Gargano, Italy	0.040	1.67	low
2	Liguria and the Côte d'Azur	0.047	1.96	low
15	North Aegean Sea	0.047	1.96	low
6	East Sicily and Messina Straits	0.096	4.0	intermediate
11	Cyclades Islands	0.113	4.71	intermediate
8	Eastern Adriatic Sea	0.119	4.96	intermediate
16	Sea of Marmara	0.126	5.25	intermediate
5	Tyrrhenian Calabria	0.127	5.29	intermediate
18	Levantine Sea	0.127	5.29	intermediate
1	Alboran Sea	0.134	5.58	intermediate
4	Aeolian Islands	0.134	5.58	intermediate
14	Eastern Aegean Sea	0.142	5.92	intermediate
9	Western Hellenic arc	0.199	8.29	high
10	Eastern Hellenic arc	0.223	9.29	high
12	Gulf of Corinth	0.308	12.83	very high

Note: H_a = absolute potential, H = normalized potential. Very low potential has been tentatively assigned to Campania, Ionian Apulia and Calabria, the central and northern Ionian Sea, the Maliakos Gulf, and Cyprus. See text for further discussion.

Risk Mitigation Technology

Tsunami risk mitigation can be achieved through a series of actions including:

1. the operation of instrumental early warning systems;
2. the construction of breakwaters;
3. the development of risk mapping using GIS tools;
4. the implementation of dedicated civil protection plans and public education.

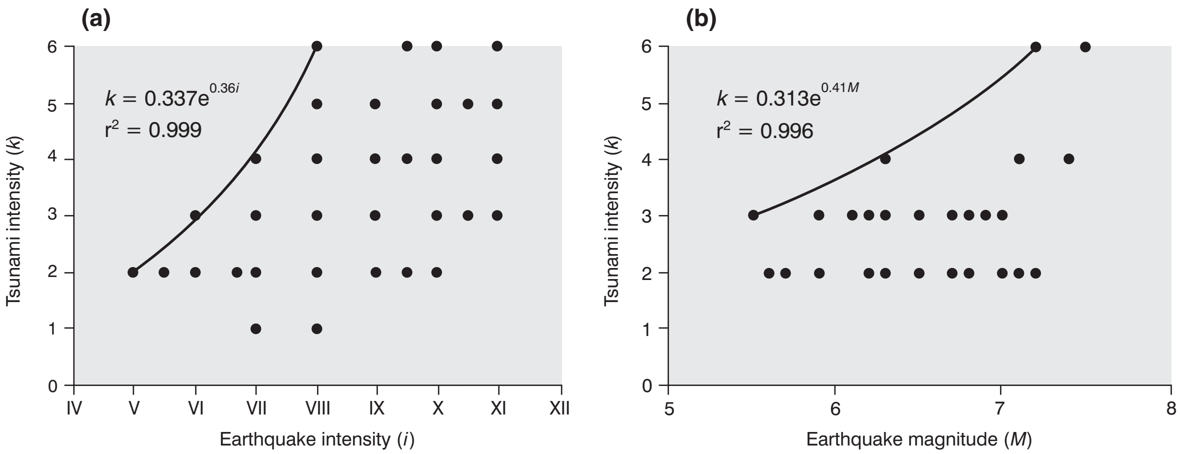

Fig. 17.16. Tsunami intensity (*k*) as a function of earthquake intensity and earthquake magnitude for the entire Mediterranean Sea database. Upper bounding envelopes are shown.

Although the countries bordering the Mediterranean Sea do not have an established tradition in this field (in contrast to Japan, for example, and other circum-Pacific countries), significant progress has been made over the last fifteen years or so. For example, experimental tsunami warning systems, consisting of both seismic and tide-gauge instruments, have recently been tested in the Messina Straits and the southern Aegean Sea (Piscini *et al.* 1998, Papadopoulos, 2003*c*). After the strong tsunami of 30 December 2002 in Stromboli, the civil protection authorities established a local tsunami alarm system. A major problem, however, for tsunami risk mitigation in the Mediterranean Sea is that travel times from tsunami sources to threatened coastal communities are short, ranging from a few minutes to around one hour depending on the source location. However, operationally viable systems can be achieved by minimizing the alarm time to no more than about five minutes from the earthquake origin time.

Pilot studies of risk mapping on a microzonation basis appear to be useful for long-term planning in the mitigation of tsunami risk (Papadopoulos and Dermentzopoulos, 1998; Papathoma *et al.* 2003). In Japan, the construction of breakwaters has been used for the protection of some coastal zones from tsunami attack, but such measures have never been recommended in the Mediterranean Sea. In comparison to other natural hazards in the Mediterranean such as earthquakes, volcanoes, and large fluvial floods, there has only been limited progress to date in the development of civil protection plans and raising public awareness of the potential threat from tsunamis in the region. While public awareness of the tsunami hazard more generally has undoubtedly been raised following the catastrophic tsunami in the Indian Ocean in December 2004, awareness of the extent of the local tsunami threat in the Mediterranean region is still rather limited. Progress in the types of action outlined above is very important for the development of an effective tsunami risk mitigation policy for the Mediterranean Sea coasts.

Using tsunami-wave simulations generated from mathematical models, Lorito *et al.* (2008) have calculated a range of parameters including wave height profiles and wave travel times to assess the potential threats to southern Italy from tsunamis generated by earthquakes in three different source zones, namely the southern Tyrrhenian thrust belt, the Tell-Atlas thrust belt, and the western Hellenic arc. The outcomes show a highly variable impact for tsunamis produced in the different source zones and this analysis highlights the need for scenario testing to be undertaken at the scale of the entire Mediterranean basin (Lorito *et al.* 2008).

Concluding Remarks

Segments of the Mediterranean Sea coast have been struck in the past by large, destructive tsunamis generated by submarine earthquakes and volcanic eruptions (e.g. Soloviev *et al.* 2000), while powerful tsunamis have also been locally generated by landslides (e.g. Papadopoulos, 1993*b*). The recurrence interval for tsunami intensities $\geq$ 4, 5, and 6 is of the order of 12, 40, and 130 years respectively. In this chapter, the highest tsunami potential has been calculated in the Hellenic arc and the Gulf of Corinth. However, infrequent but large events have been recognized for the Cyclades in the southern Aegean Sea and the Straits of Messina in southern Italy, as well as in the Alboran, Levantine, and Marmara Seas. It is clear, therefore, that tsunami waves should not be neglected as a potential source of risk that threaten coastal communities of the Mediterranean.

Several approaches offer considerable potential to improve our understanding of the tsunami phenomena and associated hazards including the identification of earthquake, volcanic eruption, and landslide sources and mechanisms as well as palaeotsunami investigations. To improve tsunami risk assessment, more work is needed to extend the event database, to simulate wave generation, propagation, and coastal inundation using numerical models and to map the components of physical and anthropogenic risk with the use of GIS tools. Recent events in south-east Asia and the Indian Ocean margins have highlighted the importance of developing risk mitigation strategies that include public awareness activities, the development of instrumental tsunami warning systems and the elaboration of specific civil protection plans across the Mediterranean region.

References

Ambraseys, N. N. (1960), The seismic sea wave of July 9, 1956, in the Greek Archipelago. *Journal of Geophysical Research* 65: 1257–65.

——(1962), Data for the investigation of the seismic sea-waves in the eastern Mediterranean. *Bulletin of the Seismological Society of America* 52: 895–913.

——(1965), The seismic history of Cyprus. *Revue pour l'étude des Calamites* 40: 25–48.

——Melville, C. P., and Adams, R. D. (1994), *The Seismicity of Egypt, Arabia and the Red Sea: A Historical Review*. Cambridge University Press, Cambridge.

Antonopoulos, J. (1979), Catalogue of tsunamis in the eastern Mediterranean from antiquity to present times. *Annali di Geofisica* 32: 113–30.

Assier-Rzadkiewicz, S., Heinrich, P., Sabatier, P.C., Sovoye, B., and Bourillet, J. F. (2000), Numerical modelling of a landslide-generated tsunami—the 1979 Nice event. *Pure and Applied Geophysics* 157: 1707—27.

Cita, M. B., and Aloisi, G. (2000), Deep-sea tsunami deposits triggered by the explosion of Santorini (3500 years BP), eastern Mediterranean. *Sedimentary Geology* 135: 181–203.

Darawcheh, R., Sbeinati, M. R., Margottini, C., and Paolini, S. (2000), The 9 July 551 AD Beirut earthquake, Eastern Mediterranean region. *Journal of Earthquake Engineering* 4: 403–14.

Dominey-Howes, D. (1996), Sedimentary deposits associated with the July 9th 1956 Aegean Sea tsunami. *Physics and Chemistry of the Earth* 21: 51–5.

——(2004), A re-analysis of the Late Bronge Age eruption and tsunami of Santorini, Greece, and the implications for the volcano-tsunami hazard. *Journal of Volcanology and Geothermal Research* 130: 107–32.

——Dawson, A., and Smith, D. (1998), Late Holocene coastal tectonics at Falasarna, W. Crete: a sedimentary study, in C. Vita-Finzi (ed.), *Coastal Tectonics*, Special Publication 146. Geological Society, London, 343–52.

——Papadopoulos, G. A., and Dawson, A.G. (2000), Geological and historical investigation of the 1650 Mt. Columbo (Thera Island) eruption and tsunami, Aegean Sea, Greece. *Natural Hazards* 21: 83–96.

Eva, C., and Rabinovich, A. B. (1997), The February 23, 1887 tsunami recorded on the Ligurian coast, western Mediterranean. *Geophysical Research Letters* 24: 2211–14.

Fokaefs, A., and Papadopoulos, G. A. (2007), Tsunami hazard in the Eastern Mediterranean: strong earthquakes and tsunamis in Cyprus and the Levantine Sea. *Natural Hazards* 40: 503–26.

Francaviglia, V. (1990), Sea-borne pumice deposits of archaeological interest on Aegean and eastern Mediterranean beaches, in D. A. Hardy *et al.* (eds.), *Thera and the Aegean World III*. Thera Foundation, London, iii. 127–34.

Fukao, Y. (1979), Tsunami earthquakes and subduction processes near deep-sea trenches. *Journal of Geophysical Research* 84: 2303–14.

Galanopoulos, A. G. (1957), The seismic sea wave of July 9, 1956. *Praktika Akadimias Athinon* 32: 90–101.

——(1960), Tsunamis observed on the coasts of Greece from Antiquity to present time. *Ann. di Geof.* 13: 369–86.

——Delibasis, N., and P. Comninakis, P. (1964), A tsunami generated by an earth slump set in motion without shock. *Annales Geologic Pays Hellenic* 16: 93–110.

Guidoboni, E., and Comastri, A. (1997), The large earthquake of 8 August 1303 in Crete: seismic scenario and tsunami in the Mediterranean area. *Journal of Seismology* 1: 55–72.

——Comastri, A., and Traina, G. (1994), *Catalogue of Ancient Earthquakes in the Mediterranean Area up to the 10th Century*. Istituto Nazionale di Geofisica, Rome.

Gutenberg, B., and Richter, C. (1944), Frequency of earthquakes in California. *Bulletin of the Seismological Society of America* 34: 185–8.

Heiken, G., and McCoy Jr., F. (1984), Caldera development during the Minoan eruption, Thira, Cyclades, Greece. *Journal of Geophysical Research* 89: 8441–62.

Imamura, A. (1937), *TheoreticaI and Applied Seismology*. Maruzen, Tokyo.

IOC (Intergovernmental Oceanographic Commission) (1998), *Post-tsunami Survey Field Guide*. 1st edn. Manuals and Guides 37. UNESCO.

Kanamori, H. (1972), Mechanism of tsunami earthquakes. *Physics of Earth and Planetary Interiors* 6: 346–59.

Kastens, K. A., and Cita, M. B. (1981), Tsunami-induced transport in the abyssal Mediterranean *Bulletin of the Geological Society of America* 92: 845–57.

Keller, J. (1978), Prehistoric pumice tephra on Aegean islands, in C. Doumas (ed.), *Thera and the Aegean World II*. Thera Foundation, London, ii. 49–56.

Koutitas, C. G., and Papadopoulos, G. A. (1998), Numerical simulation of the aseismically induced tsunami of 7 February 1963 in the Western Corinthos Bay. *Proceedings of the International Conference on Tsunamis, Paris, 26–8 May*, 247–54.

Lorito, S., Tiberti, M. M., Basili, R. Piatanesi, A., and Valensise. G. (2008), Earthquake-generated tsunamis in the Mediterranean Sea: Scenarios of potential threats to Southern

Italy. *Journal of Geophysical Research* 113, B01301, doi: 10.1029/2007JB004943.

McCoy, F. W., and Heiken, G. (2000), Tsunami generated by the Late Bronze Age eruption of Thera (Santorini), Greece. *Pure and Applied Geophysics* 157: 1227–56.

Marinatos, S. (1939), The volcanic destruction of Minoan Crete. *Antiquity* 13: 425–39.

Marinos, G., and Melidonis, N. (1971), On the strength of seaquakes (tsunamis) during the prehistoric eruptions in Santorini, in *Proceedings of the 1st International Scientific Congress on the Volcano of Thera, Athens, 15–23 September 1969*, 277–88.

Minoura, K., Imamura, F., Kuran, U., Nakamura, T., Papadopoulos, G. A., Takahashi, T.,and Yalçiner, A. C. (2000), Discovery of Minoan tsunami deposits. *Geology* 28: 59–62.

Monserrat, S., Ibbetson, A., and Thorpe, A. J. (1991), Atmospheric gravity waves and the 'Rissage' phenomenon, *Quarterly Journal of the Royal Meteorological Society* 117: 553–70.

Murty, T. S. (1977), Seismic Sea Waves–Tsunamis. *Bulletin of the Fisheries Research Board Canada* 198: 1–337.

—— and Loomis, H. G. (1980), A new objective tsunami magnitude scale. *Marine Geodesy* 4: 267–82.

Neri, G., Barberi, G., Oliva, G., and Orecchio, B. (2004), Tectonic stress and seismogenic faulting in the area of the 1908 Messina earthquake, south Italy. *Geophysical Research Letters* 31: 1–5.

Au: Please check "?" meant for?

Papadopoulos, G. A. (1993*a*), On some exceptional seismic (?) sea-waves in the Greek Archipelago. *Science of Tsunami Hazard*, 11, 25–3.

—— (1993*b*), Seismic faulting and non-seismic tsunami generation in Greece. *Proceedings of the IUGG/IOC International Tsunami Symposium, Wakayama, Japan 23–7 August, 1993*, 115–22.

—— (1998), A reconstruction of the 373 B.C. large earthquake in the western Corinthos Gulf. *Proceedings of the 2nd International Conference on Ancient Eliki, Aeghion, Athens, 1–3 Dec. 1995*, 479–94.

—— (2001), Tsunamis in the East Mediterranean: A catalogue for the area of Greece and adjacent seas. *Proceedings of the Workshop on Tsunami Risk Assessment Beyond 2000: Theory, Practice, Plans. Moscow, 14–16 June 2000*, 34–42.

—— (2003*a*), Quantification of tsunamis: a review, in A. C. Yalçiner *et al.* (eds.), *Submarine Landslides and Tsunamis*. Kluwer, Dordrecht, 285–91.

—— (2003*b*), Tsunami hazard in the Eastern Mediterranean: Strong earthquakes and tsunamis in the Corinth Gulf, Central Greece. *Natural Hazards* 29: 437–64.

—— (2003*c*), A tsunami warning system in the SW Aegean Sea, Greece, in J. Zschau and A. N. Küppers (eds.), *Early Warning Systems for Natural Disaster Reduction*. Springer, New York, 549–52.

—— and Chalkis, B. G. (1984), Tsunamis observed in Greece and the surrounding area from antiquity up to present times. *Marine Geology* 56: 309–17.

—— and Dermentzopoulos, Th. (1998), A tsunami risk management pilot study in Heraklion, Crete Isl. Greece. *Natural Hazards* 18: 91–118.

—— and Imamura, F. (2001), A proposal for a new tsunami intensity scale. *Proceedings of the International Tsunami Symposium 2001, Seattle, 7–10 August*, 569–77.

—— and Kortekaas, S. (2003), Characterisics of landslide gererated tsunamis from observational data, in L. Locat and J. Mienert (eds.), *Submarine Mass Movements and their Consequences*. Kluwer, Dordrecht, 367–74.

—— and Pavlides, S. B. (1992), The large 1956 earthquake in the South Aegean: Macroseismic field configuration, faulting, and neotectonics of Amorgos island. *Earth and Planetary Science Letters* 113: 383–96.

—— and Vassilopoulou, A. (2001), Historical and archaeological evidence of earthquakes and tsunamis felt in the Kythira strait, Greece, in G. T. Hebenstreit (ed.), *Tsunami Research at the End of a Critical Decade*. Kluwer, Dordrecht, 119–38.

—— —— and Plessa, A. (2000), A new catalogue of historical earthquakes and tsunamis in the Corinth rift, Central Greece: 480B.C.–A.D. 1910, in G. A. Papadopoulos (ed.), *Historical Earthquakes and Tsunamis in the Corinth Rift, Central Greece*. Publication 12, Institute of Geodynamics, National Observatory of Athens, 9–119.

—— Imamura, I., Minoura, K., Takahashi, T., Kuran, U., and Yalciner, A. (2004), Strong earthquakes and tsunamis in the East Hellenic Arc. *Geophysical Research Abstracts* 6: 3212.

—— —— —— —— Karakatsanis, S., Fokaefs, A., Orfanogiannaki, K., Daskalaki E., and Diakogianni, G. (2005), The 9 July 1956 large tsunami in the south Aegean Sea: compilation of a data basis and re-evaluation, in G. A. Papadopoulos and K. Satake (eds.), *Proceedings of the 22nd International Tsunami Symposium, Chania, 27–9 June*, 173–80.

Papadopoulos, G. A., Daskalaki, E., and Fokaefs, A. (2007*a*), Tsunamis generated by coastal and submarine landslides in the Mediterranean Sea, in V. Lykousis, D. Sakellariou, and J. Locat (eds.), *Submarine Mass Movements and their Consequences*. Advances in Natural and Technological Hazards Research 27. Springer, Dordrecht, 415–22.

—— —— —— and Giraleas, N. (2007*b*), Tsunami hazards in the Eastern Mediterranean: strong earthquakes and tsunamis in the East Hellenic Arc and Trench system. *Natural Hazards and Earth System Sciences* 7: 57–64.

Papaioannou, I., Papadopoulos, G. A., and Pavlides, S. (2004), The earthquake of 426B.C. in N. Evoikos Gulf revisited: amalgamation of two different strong earthquake events? *Bulletin of the Geological Society of Greece* 36: 1477–81.

Papathoma, M., Dominey-Howes, D., Zong, Y., and Smith, D. (2003), Assessing tsunami vulnerability, an example from Herakleio, Crete. *Natural Hazards and Earth System Sciences* 3: 1–13.

Papazachos, B. C., Koutitas, C. H., Hatzidimitriou, M. P., Karacostas, G. B., and Papaioannou, A. Ch. (1985), Source and short-distance propagation of the July 9, 1956 southern Aegean tsunami. *Marine Geology* 65: 343–51.

Pararas-Carayannis, G. (1992), The tsunami generated from the eruption of the volcano of Santorini in the Bronge Age. *Natural Hazards* 5: 115–23.

Patacca, E., and Scandone, P. (2004), The 1627 Gargano earthquake (Southern Italy): Identification and characterization of the causative fault. *Journal of Seismology* 8: 259–73.

Perissoratis, C., and Papadopoulos, G. A. (1999), Sediment instability and slumping in the southern Aegean Sea and the case history of the 1956 tsunami. *Marine Geology* 161: 287–305.

Pirazzoli, P. A., Ausseil-Badie, J., Giresse, P., Hadjidaki, E., and Arnold, M. (1992), Historical environmental changes at Phalasarna harbour, west Crete. *Geoarchaeology* 7: 371–92.

Piscini, A., Maramai, A., and S. Tinti (1998), Pilot local tsunami warning system in Augusta, Eastern Sicily, Italy. *International Conferernce on Tsunamis, Paris, May 26–8 1998*, 137–48.

Rothaus, R. M., Reinhardt, E., and Noller, J. (2004), Regional considerations of coastline change, tsunami damage and recovery along the southern coast of the bay of Izmit—the Kocaeli (Turkey) earthquake of 17 August 1999. *Natural Hazards* 31: 233–52.

Shuto, N. (1993), Tsunami intensity and disasters, in S. Tinti (ed.), *Tsunamis in the World*. Kluwer, Dordrecht, 197–216.

Sigurdsson, H., Carey, S., and Devine, J. D. (1990), Assessment of mass, dynamics and environmental effects of the Minoan eruption of Santorini volcano, in: D. A. Hardy *et al.* (eds.), *Thera and the Aegean World III*. Thera Foundation, London, ii. 100–12.

Soloviev, S. L. (1970), Recurrence of tsunamis in the Pacific, in W. M. Adams (ed.), *Tsunamis in the Pacific Ocean*. East–West Center Press, Honolulu, 149–63.

—— Solovieva, O., Go, C., Kim, K., and Shchetnikov, A. (2000), *Tsunamis in the Mediterranean Sea 2000 B.C. to 2000 A.D.* Kluwer, Dordrecht.

Soren, D. (1988), The day the world ended at Kourion—Reconstructing an ancient earthquake. *National Geographic*, July, 30–53.

Thommeret, Y., Thommeret, J., Laborel, J., Montaggioni, L. F., and Pirazzoli, P. A. (1981), Late Holocene shoreline changes and seismo-tectonic displacements in western Crete (Greece). *Zeitschrift für Geomorphologie*, Suppl. 40: 127–49.

Tinti, S., and Guidoboni, E. (1988), Revision of the tsunamis occurred in 1783 in Calabria and Sicily (Italy). *Science of Tsunami Hazards* 6: 17–22.

—— and Maramai, A. (1996), Catalogue of tsunamis generated in Italy and in Côte d'Azur, France: a step towards a unified catalogue of tsunamis in Europe. *Annali di Geofisica* 39: 1253–99.

—— Maramai, A., and Favali, P. (1995), The Gargano promontory: An important Italian seismogenic-tsunamigenic area. *Marine Geology* 122: 227–41.

—— —— —— (2001), Contribution of tsunami data analysis to constrain the seismic source: the case of the 1693 eastern Sicily earthquake. *Journal of Seismology* 5: 41–61.

—— —— and Graziani, L. (2004), The new catalogue of Italian tsunamis. *Natural Hazards* 33: 439–65.

Valensise, G., and Pantosti, D. (1992), A 125 kyr-long geological record of seismic source repeatability: the Messina Straits (southern Italy) and the 1908 earthquake (M_s $7^1/_2$). *Terra Nova* 4: 472–83.

Van Dorn, W. G. (1968), Tsunamis. *Contemporary Physics* 9: 145–64.

Whelan, F., and Kelletat, D. (2002), Geomorphic evidence and relative and absolute dating results for tsunami events on Cyprus. *Science Tsunami Hazards* 20: 3–18.

Yalçiner, A. C., Kuran, U., Akyarli, A., and Imamura, F. (1993), An investigation on the propagation of tsunamis in the Aegean sea by mathematical modeling, in *Proceedings of the IUGG/IOC International Tsunami Symposium, Wakayama, 23–7 August*, 65–75.

—— Alpar, B., Altinok, Y., Özbay, I., and Imamura, F. (2002), Tsunamis in the Sea of Marmara—Historical documents for the past, models for the future. *Marine Geology* 190: 445–63.

View publication stats